A novel approach for processing GNSS multi-systems/multi-frequencies for geodesy and remote sensing applications

George Hajj
Yoaz Bar-Sever
Mark Miller

Jet Propulsion Laboratory, California Institute of Technology

ION GNSS+ 2016, Portland, Oregon

© 2016 California Institute of Technology. Government sponsorship acknowledged.

Scope of The Talk

- Present a unified approach for dealing with multiple GNSS systems and multiple frequencies
- Present a new approach for solving line-of-sight total-electron content
- Evaluate this new approach in a global network scenario
- Evaluate the new approach in a regional network and impact on rapid integer bias-fixing and single frequency users

GPS Observables

$$L_1 = \rho - a\,\frac{TEC}{f_1^2} + b_{1,tr} + b_{1,rc} + n_1\,\lambda_1$$

$$L_2 = \rho - a\,\frac{TEC}{f_2^2} + b_{2,tr} + b_{2,rc} + n_2\,\lambda_2$$

$$P_1 = \rho + a\,\frac{TEC}{f_1^2} + B_{1,tr} + B_{1,rc}$$

$$P_2 = \rho + a\,\frac{TEC}{f_2^2} + B_{2,tr} + B_{2,rc}$$

Traditionally, we form the ionospheric free linear combination

$$\begin{aligned} LC &= \frac{f_1^2}{f_1^2 - f_2^2} L_1 - \frac{f_2^2}{f_1^2 - f_2^2} L_2 \\ &= \rho + \frac{f_1^2}{f_1^2 - f_2^2}\left(b_{1,tr} + b_{1,rc} + n_1\,\lambda_1\right) - \frac{f_2^2}{f_1^2 - f_2^2}\left(b_{2,tr} + b_{2,rc} + n_2\,\lambda_2\right) \\ PC &= \frac{f_1^2}{f_1^2 - f_2^2} P_1 - \frac{f_2^2}{f_1^2 - f_2^2} P_2 \\ &= \rho + \frac{f_1^2}{f_1^2 - f_2^2}\left(B_{1,tr} + B_{1,rc}\right) - \frac{f_2^2}{f_1^2 - f_2^2}\left(B_{2,tr} + B_{2,rc}\right) \end{aligned}$$

Users interested in the ionosphere would form the following linear combination

$$L_1 - L_2 = -a\,TEC\left(\frac{1}{f_1^2} - \frac{1}{f_2^2}\right) + \left(b_{1,tr} + b_{1,rc} + n_1\,\lambda_1\right) - \left(b_{2,tr} + b_{2,rc} + n_2\,\lambda_2\right)$$

$$P_1 - P_2 = a\,TEC\left(\frac{1}{f_1^2} - \frac{1}{f_2^2}\right) + \left(B_{1,tr} + B_{1,rc}\right) - \left(B_{2,tr} + B_{2,rc}\right)$$

Limitations of Traditional Approach

- Does not extend naturally to multiple frequencies where multiple ionospheric-free linear combinations can be formed
- The noise of an ionospheric-free linear-combination is amplified by a factor of 3-4 and is dominated by the noisier signal
- Ignores correlation of ionosphere between measurements close in time and space. This becomes specially important in regional networks or as more navigation satellites become operational

A more general approach

Approach:

- Treat all data in their raw form—i.e., no ionospheric-free linear combination
- Explicitly solve for line-of-sight TEC at each epoch as part of the state solution
- Introduce extra constraints on the spatial and temporal variability of the ionosphere

Advantages:

- Eliminates the need to a priori decide on the optimal linear combination to form
- Reduce the noise introduced by the ionospheric-free linear combination multiplier
- Accounts for the noise characteristics of each measurement type
- Utilize spatial and temporal correlation on the ionosphere to further reduce data noise
- Obtain precise slant TEC (STEC) as a bonus
- In a dense network region, solution of STEC can be used for rapid integer-bias fixing and for precise positioning of single-frequency users

Constraining the Ionospheric

$$\begin{pmatrix} TEC_1 \\ \dots \\ TEC_m \end{pmatrix} = A \begin{pmatrix} e_1 \\ \dots \\ e_n \end{pmatrix}$$

$$A = U\,S\,V^T$$

$$U = (u_1, u_2, \dots, u_m)$$

$$\begin{bmatrix} u_{r+1}^T \\ \vdots \\ u_m^T \end{bmatrix} \begin{pmatrix} TEC_1 \\ \dots \\ TEC_m \end{pmatrix} = 0$$

Representing the ionosphere by a set of voxels is one approach to introducing the spatial and temporal correlation. For *m* measurements and *n* voxels, slant TEC can be related linearly to electron densities through matrix A. By performing singular-value decomposition, we can isolate the linearly dependent set of equations which can be used as additional constraints when solving for the slant TEC.

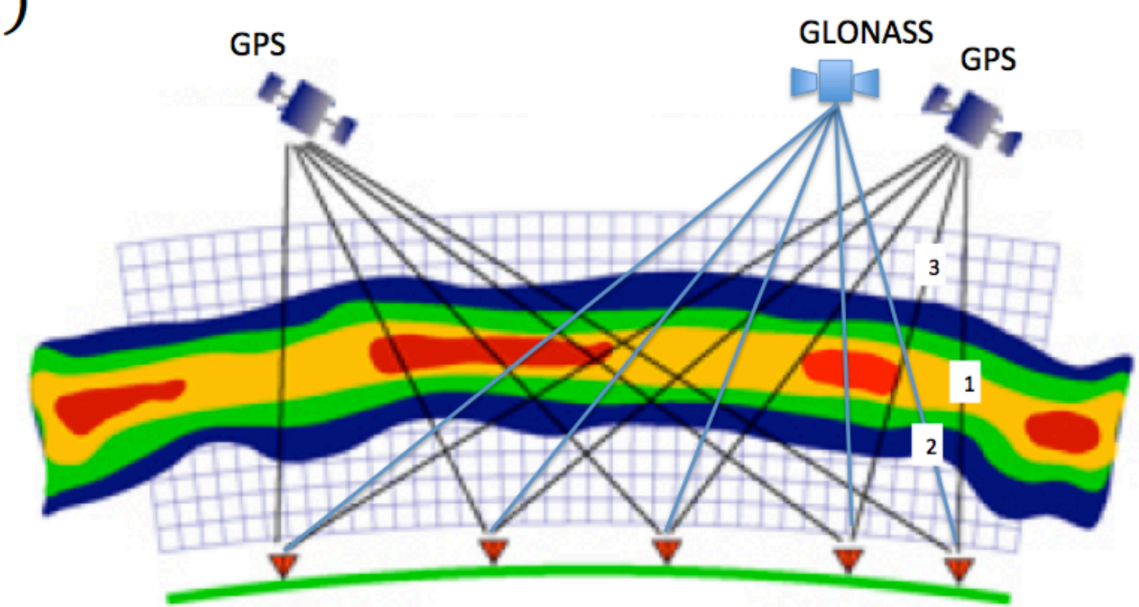

The Impact of Ionospheric Constraints in a global solution

- Process data from a global network of 80 GPS stations for a 30-hour run
- Resolve integer ambiguity by use of traditional wide-lane and narrow lanes
- Solve for double differenced—integer resolved—TEC
- Solve for slant TEC from double differenced TEC *with* and *without* introducing the ionospheric constraints

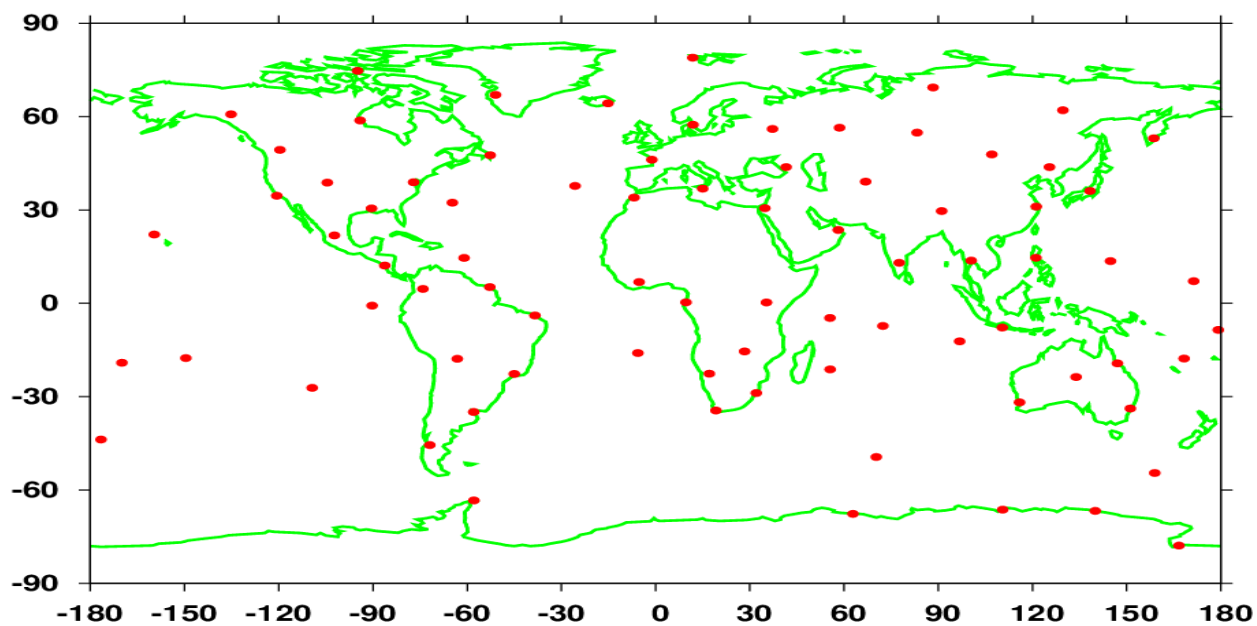

A 30-hour Run from a Global GPS Network

- Data rate: once every 5-minute
- Total number of data points: 278892
- Number of connected arcs: 6297
- Number of all double differenced links: 5198954
- ~75% of double differenced TEC are resolved to better than 0.01 from an integer

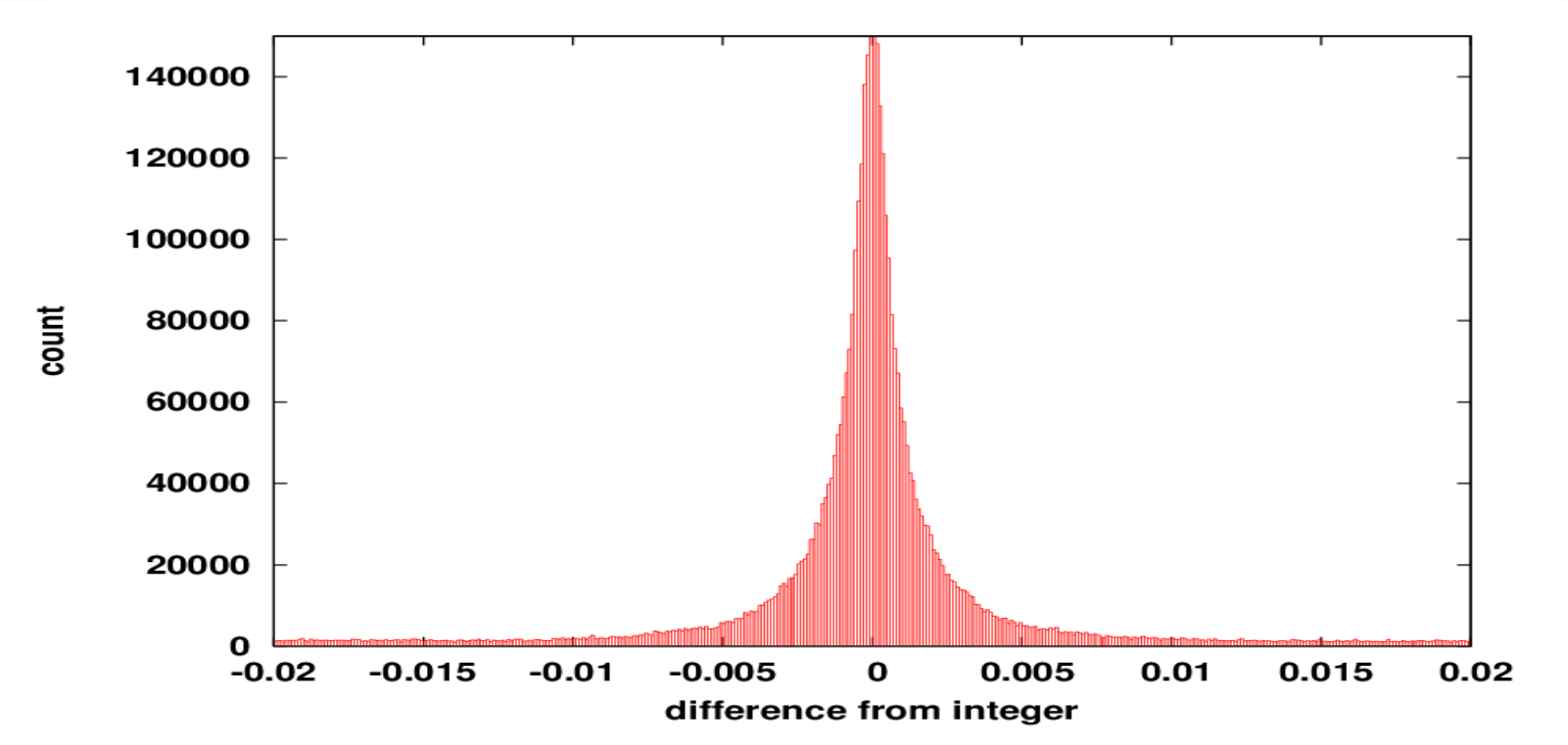

Solving for line-of-sight TEC

- Given precise integer-resolved TEC, how well can we resolve slant TEC?
- Effect of spatial constraints is seen by changing STEC solution from non-physical negative values to physical positive values
- Remaining negative STEC after constraints is an indication of ionospheric representation error

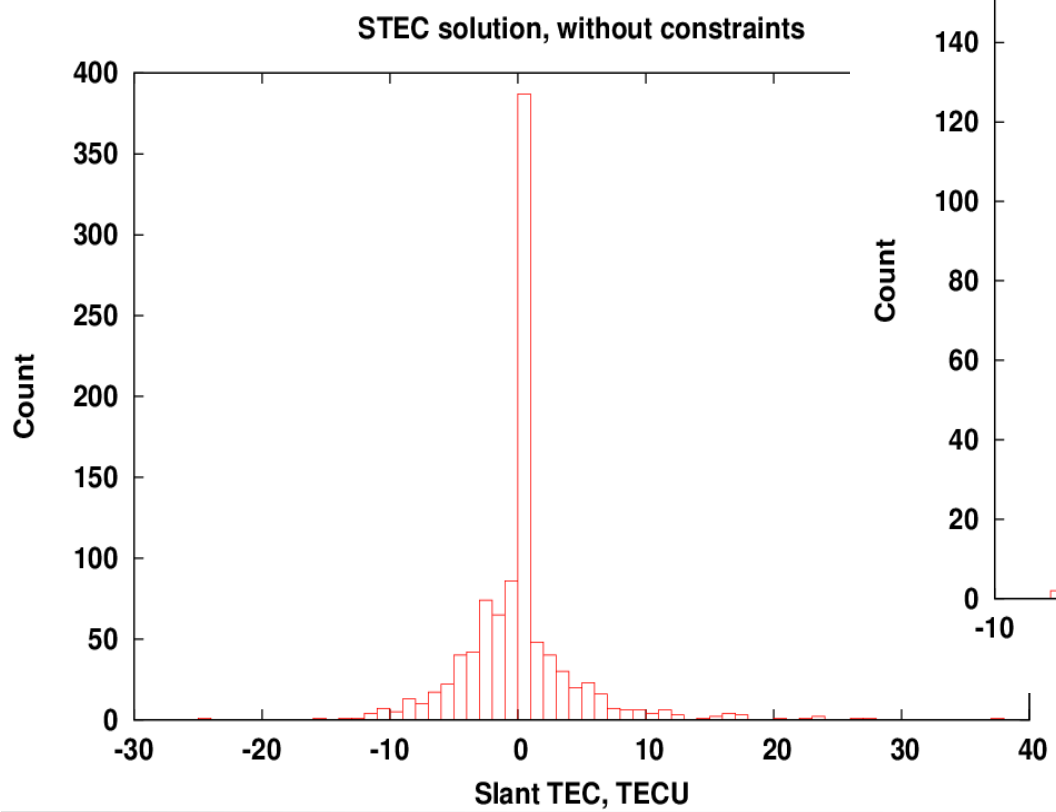

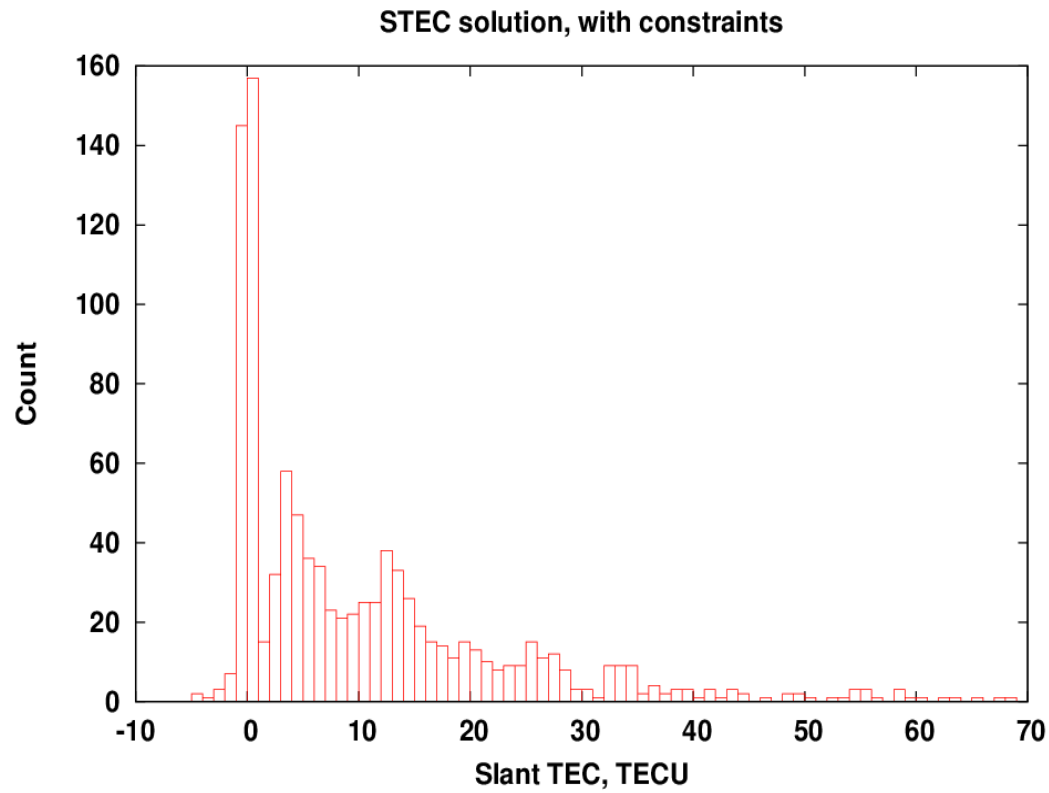

Assessment of STEC Accuracy in a regional network over Southern California

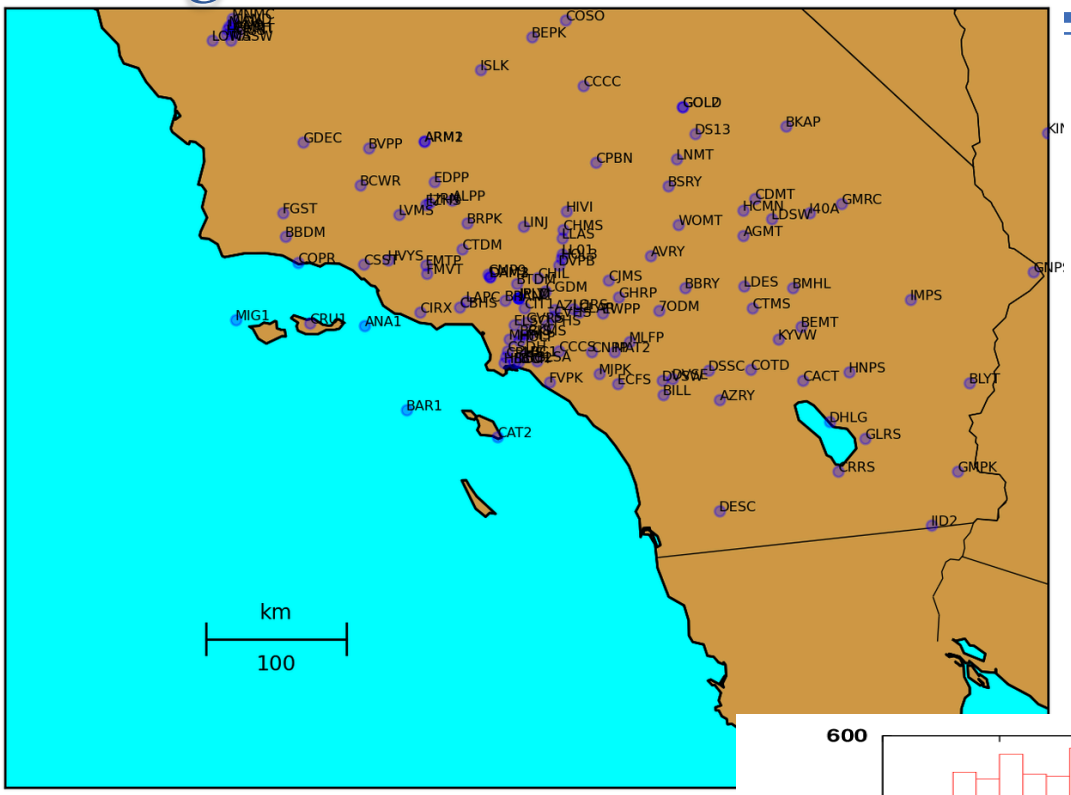

We examine the degree of correlation of the ionosphere in a regional network. Here we consider data collected on 2014-01-01 from a set of 127 stations in Southern California (left). The distribution of all possible baselines formed from this network covers a distance from 20 to 600 km (below)

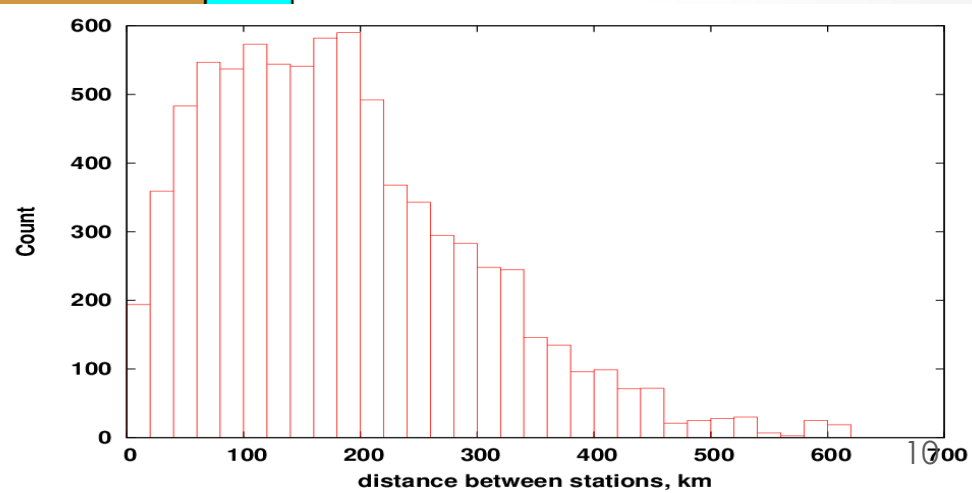

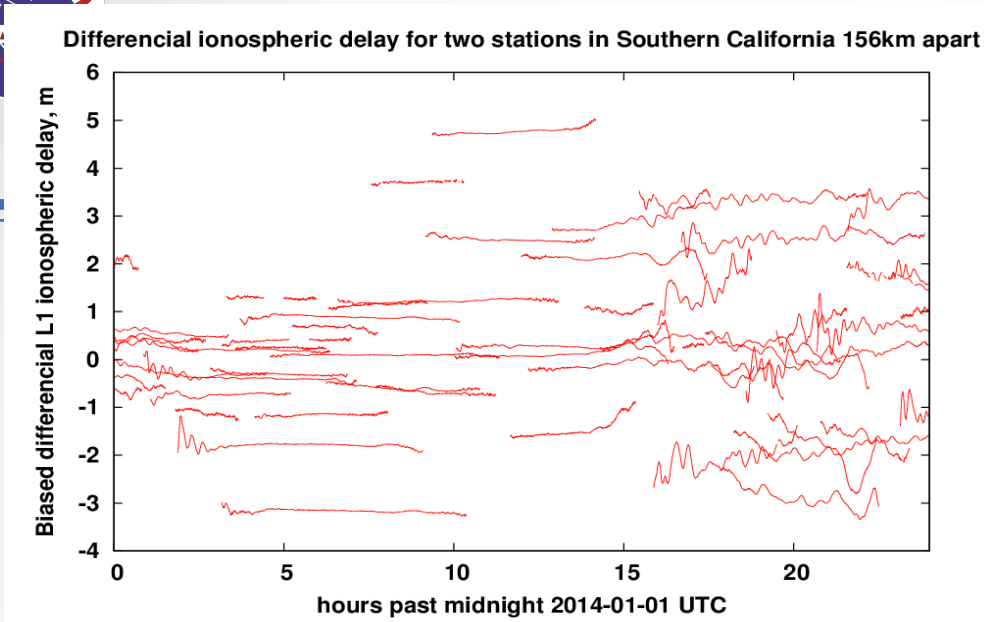

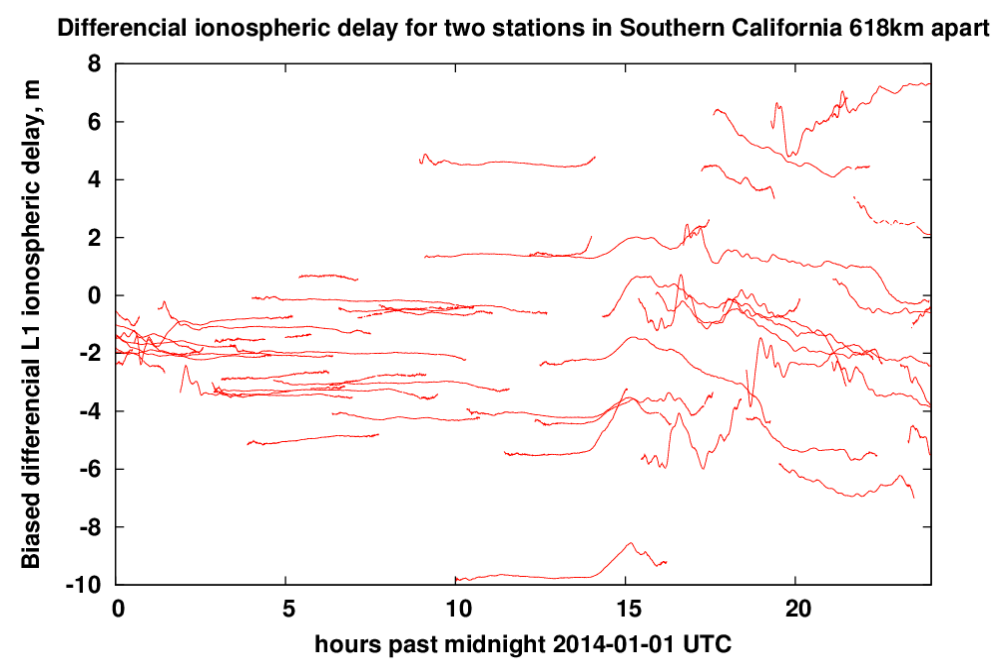

By differencing L1 and L2 phase measurements (Li) we determine the ionospheric total electron content (TEC) along a line-of-sight between a transmitter and a receiver, up to an unknown constant. Differencing Li between two receivers shows the relative difference in TEC between these two receivers, up to an unknown constant. The two figures on the left show this differential ionosphere, mapped to L1 delay, for all tracks seen by two receivers with a 156km baseline (BBDM-CAND) (top figure) and 618 km baseline (IID2-LOWS) (bottom figure). Each track can be summarized by a standard deviation (σ_{TEC}) which represents the degree of spatial variation of the ionosphere as a function of time. The small variability for tracks between hours 0-10 UTC correspond to local night-time.

Using σ_{TEC} introduced in the previous viewgraph as a proxy of the spatial variability of the ionosphere between stations, we compute σ_{TEC} for each possible pair of stations in the Southern California network for each connected arc. The distribution of σ_{TEC} is shown as a 1D histogram in the bottom figure with a mode of 1cm, a median of 2.8cm and 90 percentile of 12cm. A 2D histogram (figure to the right) shows how the tail of the distribution grows with the baseline distance.

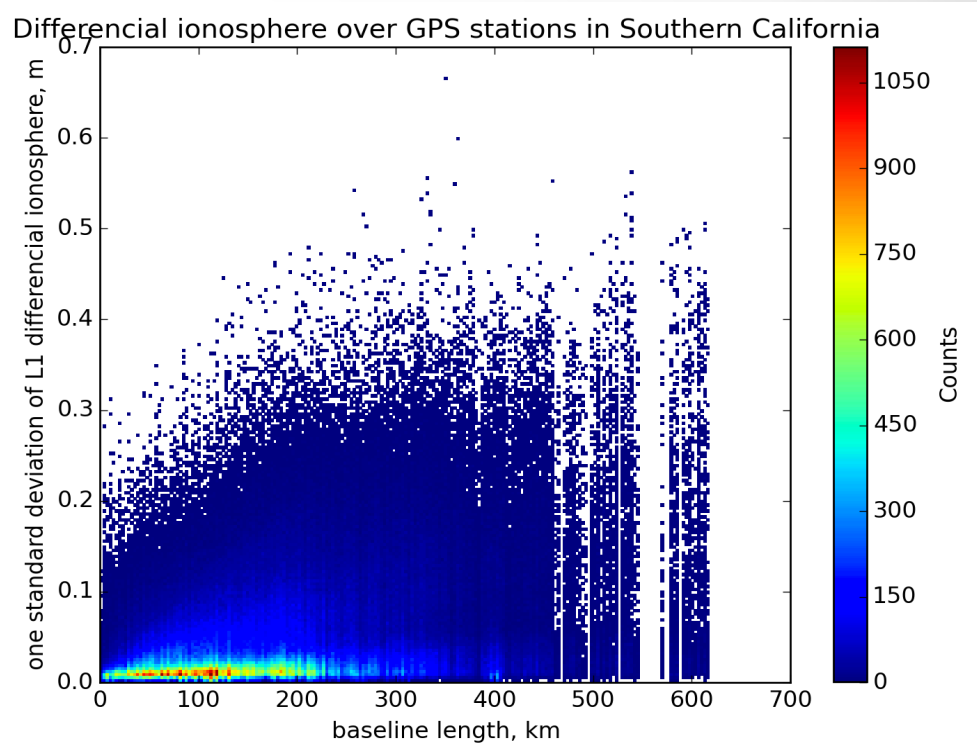

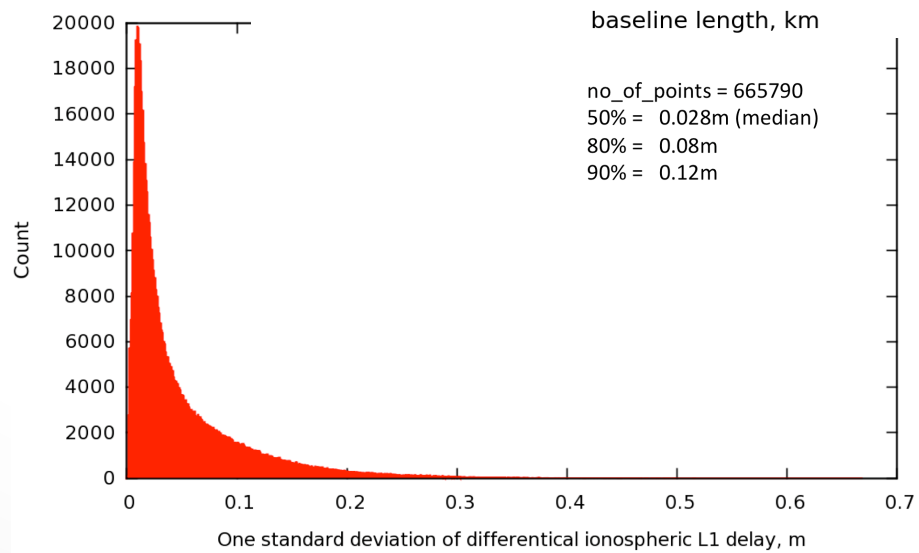

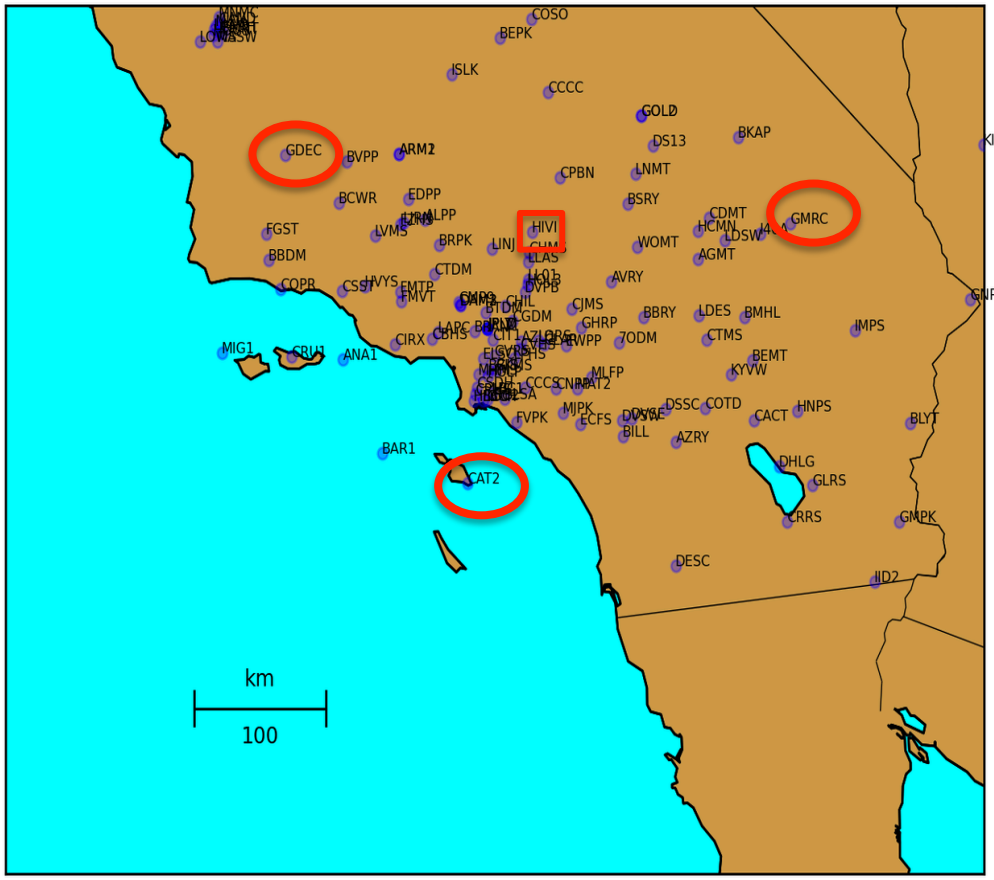

Another way of examining spatial correlation of the ionosphere is by attempting to approximate line-of-sight TEC (LTEC) at a given station by interpolation from nearby stations and comparing to the true LTEC. As a first and simple approximation, we use a triangular barycentric interpolation scheme between three "reference" stations (encircled by ellipses on the map) to interpolate to a station that lies within the triangle. A more elaborate interpolation would normally be used when more reference stations are available to capture spatial gradients of second order or higher.

In a barycentric interpolation, the value of a function V at P is the weighted average of V at the vertices according to the areas A_1, A_2 and A_3.

$$V_p = \frac{A_1 V_{x_1} + A_2 V_{x_2} + A_3 V_{x_3}}{A_1 + A_2 + A_3}$$

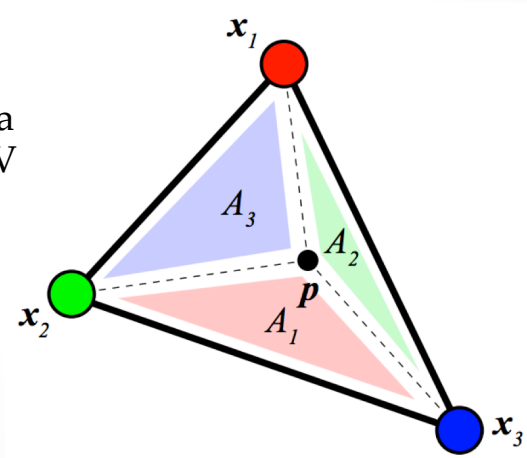

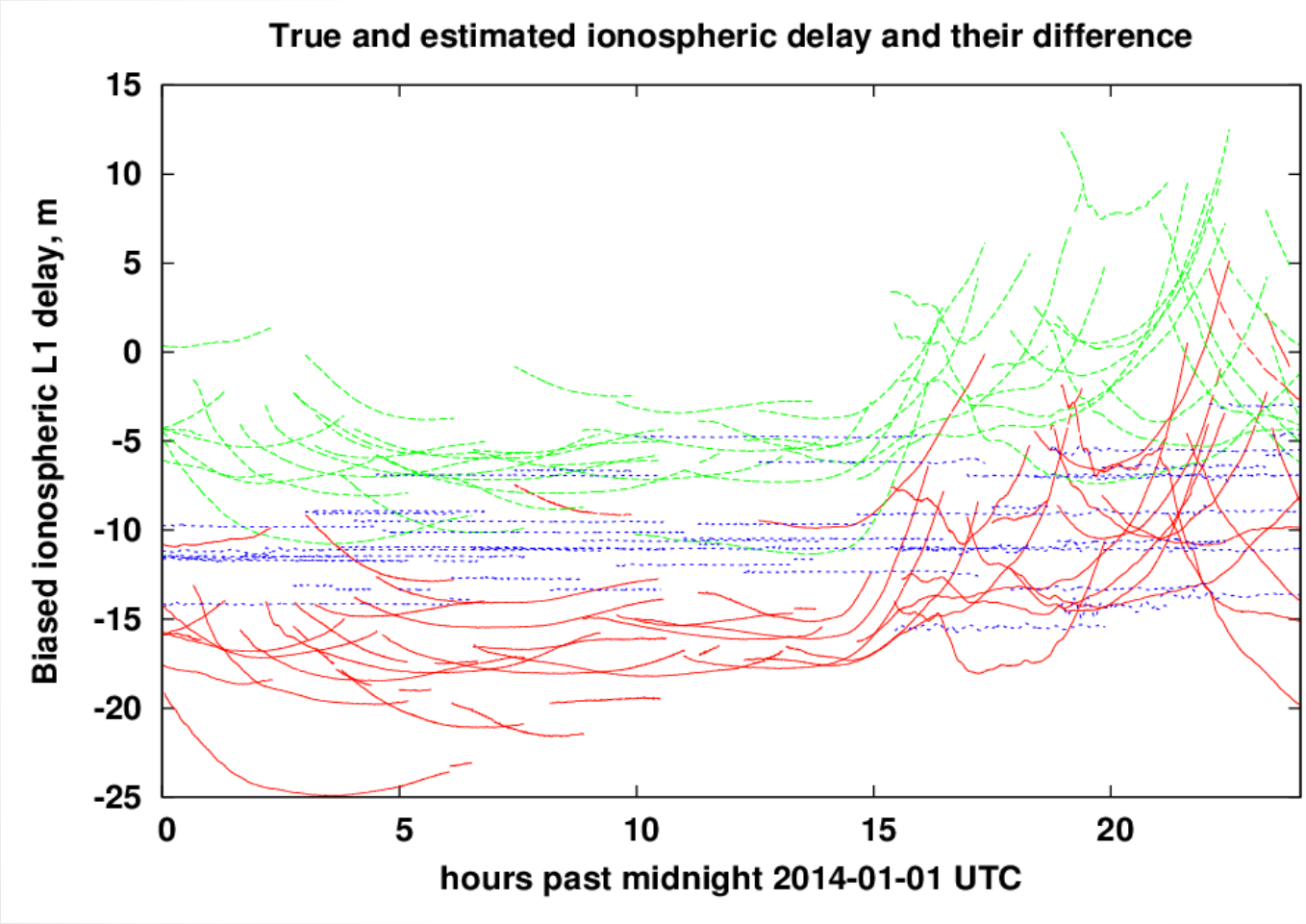

Applying the interpolation scheme introduced above using the three reference stations (GDEC, GMRC, CAT2) to the HIVI station, the plot shows the true relative TEC (red), the interpolated relative TEC (green) and their difference (blue). By use of interpolation, the ionospheric L1 delay is approximated to within a few cm.

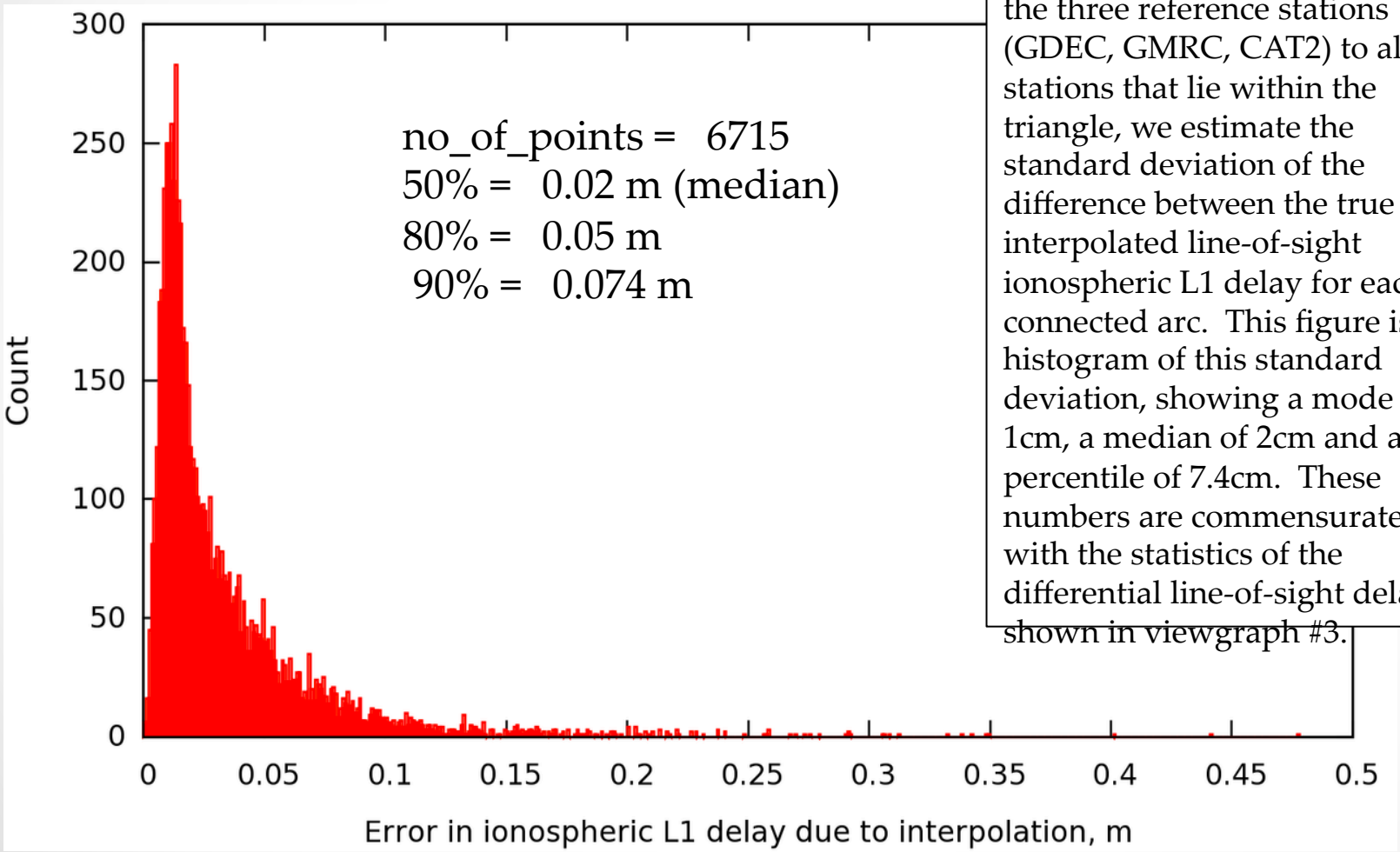

Applying the triangular barycentric interpolation using the three reference stations (GDEC, GMRC, CAT2) to all the stations that lie within the triangle, we estimate the standard deviation of the difference between the true and interpolated line-of-sight ionospheric L1 delay for each connected arc. This figure is a histogram of this standard deviation, showing a mode of 1cm, a median of 2cm and a 90 percentile of 7.4cm. These numbers are commensurate with the statistics of the differential line-of-sight delays shown in viewgraph #3.

True vs. Interpolated Double Differenced TEC

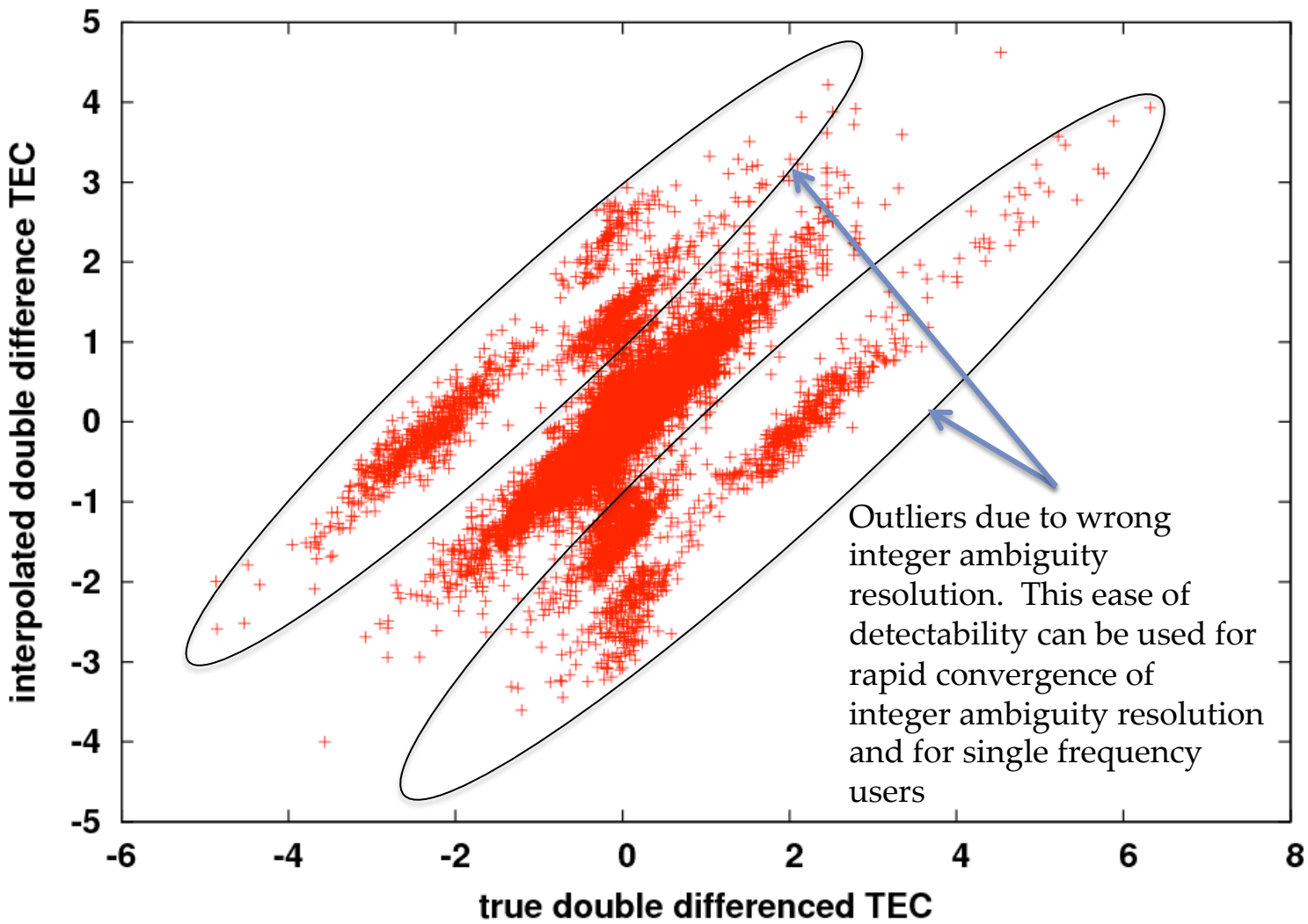
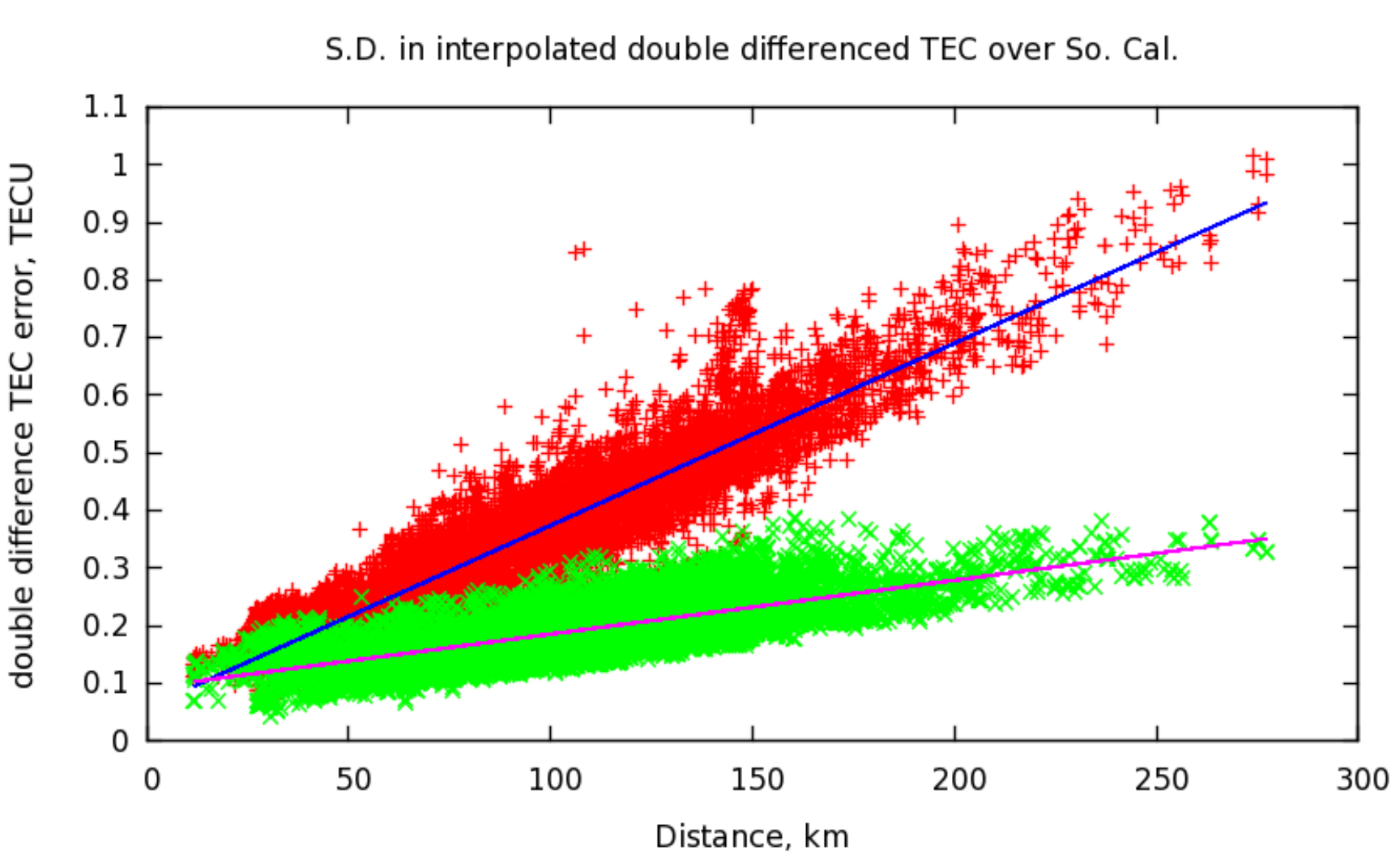
Accuracy of interpolated double differenced TEC vs. effective distance to nearby stations